



CERN-EP-2016-173
 LHCb-PAPER-2016-020
 May 19, 2017

Measurement of the ratio of branching fractions

$$\mathcal{B}(B_c^+ \rightarrow J/\psi K^+) / \mathcal{B}(B_c^+ \rightarrow J/\psi \pi^+)$$

The LHCb collaboration[†]

Abstract

The ratio of branching fractions $R_{K/\pi} \equiv \mathcal{B}(B_c^+ \rightarrow J/\psi K^+) / \mathcal{B}(B_c^+ \rightarrow J/\psi \pi^+)$ is measured with pp collision data collected by the LHCb experiment at centre-of-mass energies of 7 TeV and 8 TeV, corresponding to an integrated luminosity of 3 fb^{-1} . It is found to be $R_{K/\pi} = 0.079 \pm 0.007 \pm 0.003$, where the first uncertainty is statistical and the second is systematic. This measurement is consistent with the previous LHCb result, while the uncertainties are significantly reduced.

Published in JHEP 09(2016)153

© CERN on behalf of the LHCb collaboration, licence CC-BY-4.0.

[†]Authors are listed at the end of this paper.

1 Introduction

The B_c^+ meson, the lightest $\bar{b}c$ bound state, can only decay weakly. Since it contains only heavy quarks, its decays can be analysed using various theoretical approaches, including QCD-based methods [1–3] and QCD-inspired phenomenological models [4, 5]. A measurement of the weak decay properties of B_c^+ mesons can test these approaches and provide insight into the dynamics of the heavy quarks in the B_c^+ meson.

The exclusive decay¹ $B_c^+ \rightarrow J/\psi K^+$ is of particular interest since it proceeds via a $\bar{b} \rightarrow \bar{c}u\bar{s}$ transition and thus is CKM-suppressed by a factor $|V_{us}/V_{ud}|^2 \sim 0.05$ with respect to $B_c^+ \rightarrow J/\psi \pi^+$, where the dominant amplitude is a $\bar{b} \rightarrow \bar{c}u\bar{d}$ transition. In addition to the CKM matrix elements, the ratio of branching fractions $R_{K/\pi} \equiv \mathcal{B}(B_c^+ \rightarrow J/\psi K^+)/\mathcal{B}(B_c^+ \rightarrow J/\psi \pi^+)$ depends on the form factors of the two decays. Theoretical calculations of $R_{K/\pi}$ have been carried out using approaches that handle the non-factorisable and non-perturbative contributions in different ways, yielding values in the range from 0.05 to 0.10 [1, 5–15].

The decay $B_c^+ \rightarrow J/\psi K^+$ was first observed by the LHCb collaboration, which reported a measurement of $R_{K/\pi} = 0.069 \pm 0.019 \pm 0.005$ [16]. The uncertainty on this value is too large to discriminate between the predictions quoted above. The pp data sample used in Ref. [16], taken at a centre-of-mass energy of 7 TeV and corresponding to an integrated luminosity of 1 fb^{-1} , is now reanalysed in this paper together with an additional sample taken at a centre-of-mass energy of 8 TeV and corresponding to an integrated luminosity of 2 fb^{-1} . Owing to improvements in the analysis method as well as the increase in the data sample size, the statistical uncertainty is reduced by a factor of more than two. The systematic uncertainty is also reduced.

2 Detector and simulation

The LHCb detector [17, 18] is a single-arm forward spectrometer covering the pseudorapidity range $2 < \eta < 5$, designed for the study of particles containing b or c quarks. The detector includes a high-precision tracking system consisting of a silicon-strip vertex detector surrounding the pp interaction region, a large-area silicon-strip detector located upstream of a dipole magnet with a bending power of about 4 Tm, and three stations of silicon-strip detectors and straw drift tubes placed downstream of the magnet. The tracking system provides a measurement of charged particle momentum, p , with a relative uncertainty that varies from 0.5% at low momentum to 1.0% at 200 GeV/ c . The minimum distance of a track to a primary vertex (PV), the impact parameter, is measured with a resolution of $(15 + 29/p_T) \mu\text{m}$, where p_T (in GeV/ c) is the component of the momentum transverse to the beam direction. Different types of charged hadrons are distinguished using information from two ring-imaging Cherenkov (RICH) detectors. Photons, electrons and hadrons are identified by a calorimeter system consisting of scintillating-pad and preshower detectors, an electromagnetic calorimeter and a hadronic calorimeter. Muons are identified by a system composed of alternating layers of iron and multiwire proportional chambers.

The trigger comprises a hardware stage and a software stage. The hardware trigger employed in this analysis uses information from the muon system to select single muons

¹The inclusion of charge-conjugate processes is implied throughout the paper.

or muon pairs, applying p_T requirements. The subsequent software trigger is composed of two stages, the first of which performs a partial reconstruction and requires either a pair of well-reconstructed, oppositely charged muons having an invariant mass above $2.7 \text{ GeV}/c^2$, or a single well-reconstructed muon. The second stage of the software trigger applies a full event reconstruction, and requires at least one of the following two conditions to be fulfilled: either two opposite-sign muons must form a good-quality vertex that is well separated from all of the primary vertices and must have an invariant mass within $120 \text{ MeV}/c^2$ of the known J/ψ mass [19], or an algorithm using a boosted decision tree must identify a two- or three-track vertex that is well separated from all of the primary vertices and includes a muon among the constituent tracks. The same trigger requirements are used to select both $B_c^+ \rightarrow J/\psi K^+$ and $B_c^+ \rightarrow J/\psi \pi^+$ decays, due to the similarity in their kinematic distributions.

In the simulation, pp collisions are generated using PYTHIA 6 [20] with a specific LHCb configuration [21], or, for the hard process $gg \rightarrow B_c^+ + b + \bar{c}$ that is the dominant source of B_c^+ mesons, using the dedicated generator BCVEGPY [22,23]. Decays of hadronic particles are described by EVTGEN [24], in which final-state radiation is generated using PHOTOS [25]. The interaction of the generated particles with the detector, and its response, are implemented using the GEANT4 toolkit [26] as described in Ref. [27].

3 Event selection

Candidate $B_c^+ \rightarrow J/\psi h^+$ decays, with $J/\psi \rightarrow \mu^+\mu^-$ and h^+ being a K^+ or π^+ , are reconstructed as follows. First a loose preselection is applied. Pairs of oppositely charged, well-reconstructed muon tracks with $p_T > 550 \text{ MeV}/c$ consistent with originating from a common vertex are combined to form $J/\psi \rightarrow \mu^+\mu^-$ candidates. Hadron (h^+) candidates are selected from well-reconstructed tracks with $p_T > 500 \text{ MeV}/c$, inconsistent with originating from any PV and with the muon hypothesis. Candidate $B_c^+ \rightarrow J/\psi K^+$ and $B_c^+ \rightarrow J/\psi \pi^+$ decays are formed from $J/\psi h^+$ combinations that originate from a common vertex. They must also be within $500 \text{ MeV}/c^2$ of the known B_c^+ mass [19]. The impact parameter χ^2 , χ_{IP}^2 , which is defined as the difference in the vertex fit χ^2 of the PV with and without the particle under consideration, is required to be less than 16 for the B_c^+ candidates.

A multivariate classifier using a boosted decision tree (BDT) [28] is constructed to further suppress the combinatorial background. The kinematic variables used as inputs to the BDT are chosen to discriminate between signal and background. The twelve variables chosen are: the χ_{IP}^2 of the B_c^+ , J/ψ , μ^+ , μ^- and h^+ candidates; the p_T of the J/ψ , μ^+ , μ^- and h^+ candidates; the χ^2 per degree of freedom of the B_c^+ vertex fit; and the decay time and the decay length of the B_c^+ candidate. Since the kaon-pion mass difference is small compared with the energy release of $B_c^+ \rightarrow J/\psi h^+$ decays, the distributions of the BDT variables are similar for $B_c^+ \rightarrow J/\psi K^+$ and $B_c^+ \rightarrow J/\psi \pi^+$ decays. The BDT is trained with simulated $B_c^+ \rightarrow J/\psi \pi^+$ decays to represent both the $B_c^+ \rightarrow J/\psi K^+$ and the $B_c^+ \rightarrow J/\psi \pi^+$ signals, and with events from the upper mass sideband of the $B_c^+ \rightarrow J/\psi \pi^+$ candidates in data, $[6444, 6528] \text{ MeV}/c^2$, to represent the combinatorial background. For one third of the events in the training samples the centre-of-mass energy is 7 TeV, and for the rest it is 8 TeV in accordance with the ratio of integrated luminosities. Since the BDT does not use any particle identification information, it selects both $B_c^+ \rightarrow J/\psi K^+$

and $B_c^+ \rightarrow J/\psi \pi^+$ candidates. Particle identification requirements using information from the RICH subdetectors are then applied to the hadrons to obtain two mutually exclusive samples of $B_c^+ \rightarrow J/\psi K^+$ and $B_c^+ \rightarrow J/\psi \pi^+$ candidates.

The BDT and particle identification requirements are optimised sequentially on the sample of $B_c^+ \rightarrow J/\psi K^+$ candidates that pass the loose preselection to maximise $N_K/\sqrt{N_{\text{tot}}}$, where N_{tot} is the total number of candidates within ± 3 times the mass resolution around the known B_c^+ mass. Here N_K refers to the $B_c^+ \rightarrow J/\psi K^+$ signal yield and is estimated to be $(N_{\text{tot}} - N_{\text{comb}})/(1 + 1/(r_{\text{eff}} R_{K/\pi}))$, where the value of $R_{K/\pi}$ is taken from the previous LHCb measurement [16], N_{comb} is the number of combinatorial background events in the signal region extrapolated from the upper sideband, and r_{eff} represents the ratio of the numbers of $B_c^+ \rightarrow J/\psi K^+$ and $B_c^+ \rightarrow J/\psi \pi^+$ events that pass the $B_c^+ \rightarrow J/\psi K^+$ selection and fall in the signal window. After this optimisation, the BDT rejects more than 99.8% of the combinatorial background and keeps around 70% of $B_c^+ \rightarrow J/\psi h^+$ events. This particle identification requirement has an efficiency of about 70% for $B_c^+ \rightarrow J/\psi K^+$ and 87% for $B_c^+ \rightarrow J/\psi \pi^+$, while the probabilities for a charged kaon to be misidentified as a pion and a charged pion to be misidentified as a kaon are below 7% and 1%, respectively.

4 Signal yields and efficiency correction

The measurement is made by evaluating

$$R_{K/\pi} \equiv \frac{\mathcal{B}(B_c^+ \rightarrow J/\psi K^+)}{\mathcal{B}(B_c^+ \rightarrow J/\psi \pi^+)} = \frac{N(B_c^+ \rightarrow J/\psi K^+)}{N(B_c^+ \rightarrow J/\psi \pi^+)} \times \frac{\epsilon(B_c^+ \rightarrow J/\psi \pi^+)}{\epsilon(B_c^+ \rightarrow J/\psi K^+)}, \quad (1)$$

where $N(B_c^+ \rightarrow J/\psi K^+)$ and $N(B_c^+ \rightarrow J/\psi \pi^+)$ are the signal yields, and $\epsilon(B_c^+ \rightarrow J/\psi K^+)$ and $\epsilon(B_c^+ \rightarrow J/\psi \pi^+)$ are the total efficiencies estimated with simulation and control samples of data.

The signal yields $N(B_c^+ \rightarrow J/\psi K^+)$ and $N(B_c^+ \rightarrow J/\psi \pi^+)$ are obtained from a simultaneous unbinned maximum likelihood fit to the distribution of B_c^+ candidate masses in the range 6000 to 6600 MeV/ c^2 . These candidates include the part of the background training sample that passes the full selection; the effect of doing so has been investigated and found not to lead to any systematic bias. The fit model includes components due to signal, combinatorial background and misidentified decays ($B_c^+ \rightarrow J/\psi \pi^+$ misidentified as $B_c^+ \rightarrow J/\psi K^+$, or vice versa).

A partially reconstructed background component is included for $B_c^+ \rightarrow J/\psi \pi^+$. This background is mainly due to $B_c^+ \rightarrow J/\psi \rho^+$ decays followed by $\rho^+ \rightarrow \pi^+ \pi^0$. The data show no clear indication of partially reconstructed background for $B_c^+ \rightarrow J/\psi K^+$. A systematic uncertainty is assigned due to the non-inclusion of this background component.

The signal mass distribution of $B_c^+ \rightarrow J/\psi h^+$ is described by the sum of two double-sided Crystal Ball (F^{DSCB}) functions consisting of a Gaussian core and power law tails on both sides,

$$f_{\text{sig}}(M_{B_c^+}) = \alpha F_1^{\text{DSCB}}(M_{B_c^+}) + (1 - \alpha) F_2^{\text{DSCB}}(M_{B_c^+}), \quad (2)$$

where $M_{B_c^+}$ is the invariant mass of the $\mu^+ \mu^- h^+$ combination with the mass of the $\mu^+ \mu^-$ pair constrained to the known J/ψ mass. In the simultaneous fit, the Gaussian mean and the core mass resolution σ_1 of F_1^{DSCB} are allowed to vary, and set to be the same for both the $B_c^+ \rightarrow J/\psi \pi^+$ and the $B_c^+ \rightarrow J/\psi K^+$ decays. The tail parameters, the fraction α and

the ratio σ_2/σ_1 of the core-mass resolutions of F_1^{DSCB} and F_2^{DSCB} are fixed to the values obtained in simulation.

The combinatorial background for each decay mode is modelled by an exponential distribution. Background arising from misidentified $B_c^+ \rightarrow J/\psi h^+$ decays is described by a DSCB function, with shape and mass offset relative to the signal peak derived from simulation for each mode separately. The invariant mass distribution of the partially reconstructed background is taken to be an ARGUS function [29] convolved with a Gaussian resolution function. The mean and the width parameters of the resolution function are set to be zero and $\sqrt{\alpha\sigma_1^2 + (1-\alpha)\sigma_2^2}$.

The parameters estimated from the simultaneous fit are: the yield $N(B_c^+ \rightarrow J/\psi \pi^+)$, the yield ratio $N(B_c^+ \rightarrow J/\psi K^+)/N(B_c^+ \rightarrow J/\psi \pi^+)$, the numbers of combinatorial background events for $B_c^+ \rightarrow J/\psi K^+$ and $B_c^+ \rightarrow J/\psi \pi^+$ decays, the number of misidentification background events for each of the decay modes, the number of partially reconstructed background events for the $B_c^+ \rightarrow J/\psi \pi^+$ decay, and the shape parameters describing the signal and background distributions.

The results of the separate fits to the 7 and 8 TeV samples are shown in Fig. 1. In the 7 TeV sample, the yield $N(B_c^+ \rightarrow J/\psi \pi^+)$ is found to be 954 ± 36 and the yield ratio $N(B_c^+ \rightarrow J/\psi K^+)/N(B_c^+ \rightarrow J/\psi \pi^+)$ is found to be 0.069 ± 0.010 . The corresponding values in the 8 TeV sample are 2253 ± 53 and 0.059 ± 0.006 .

The ratio of branching fractions $R_{K/\pi}$ is obtained by correcting the yield ratio with the relative efficiency, as shown in Eq. 1. The total efficiencies include contributions from the LHCb detector acceptance and from selection, trigger and particle identification requirements. The selection and trigger efficiencies are calculated from simulated samples. The simulated events are weighted to account for differences from data in the track multiplicity distribution. It has been checked that after this weighting, the distributions of the variables used as inputs to the BDT are similar in data and simulation. The particle identification efficiencies for hadrons are evaluated from simulation calibrated with a control sample of $D^{*+} \rightarrow D^0 \pi^+$, $D^0 \rightarrow K^- \pi^+$ decays. The efficiency ratio is determined to be $\epsilon(B_c^+ \rightarrow J/\psi \pi^+)/\epsilon(B_c^+ \rightarrow J/\psi K^+) = 1.277 \pm 0.007$ and 1.284 ± 0.006 for 7 TeV and 8 TeV data, respectively. The efficiency difference between $B_c^+ \rightarrow J/\psi \pi^+$ and $B_c^+ \rightarrow J/\psi K^+$ mainly arises from particle identification for the hadrons.

5 Systematic uncertainties

Since the running conditions changed between 7 TeV and 8 TeV, the systematic uncertainties on $R_{K/\pi}$ are determined separately for the two samples. Table 1 summarises the relative systematic uncertainties associated with the mass fit and efficiency estimates that affect the ratio of branching fractions. The sources of these uncertainties are discussed below.

Each of the systematic uncertainties associated with the mass fit is studied by generating an ensemble of pseudoexperiments according to the nominal model described above and fitting them with an alternative model. The difference in the mean values of $R_{K/\pi}$ obtained is taken as the systematic uncertainty.

Changing the signal model from the sum of two DSCB functions to a single DSCB function leads to relative systematic uncertainties of 0.5% and 0.8% for the 7 TeV and 8 TeV data, respectively. Using a third-order polynomial in place of an exponential function for

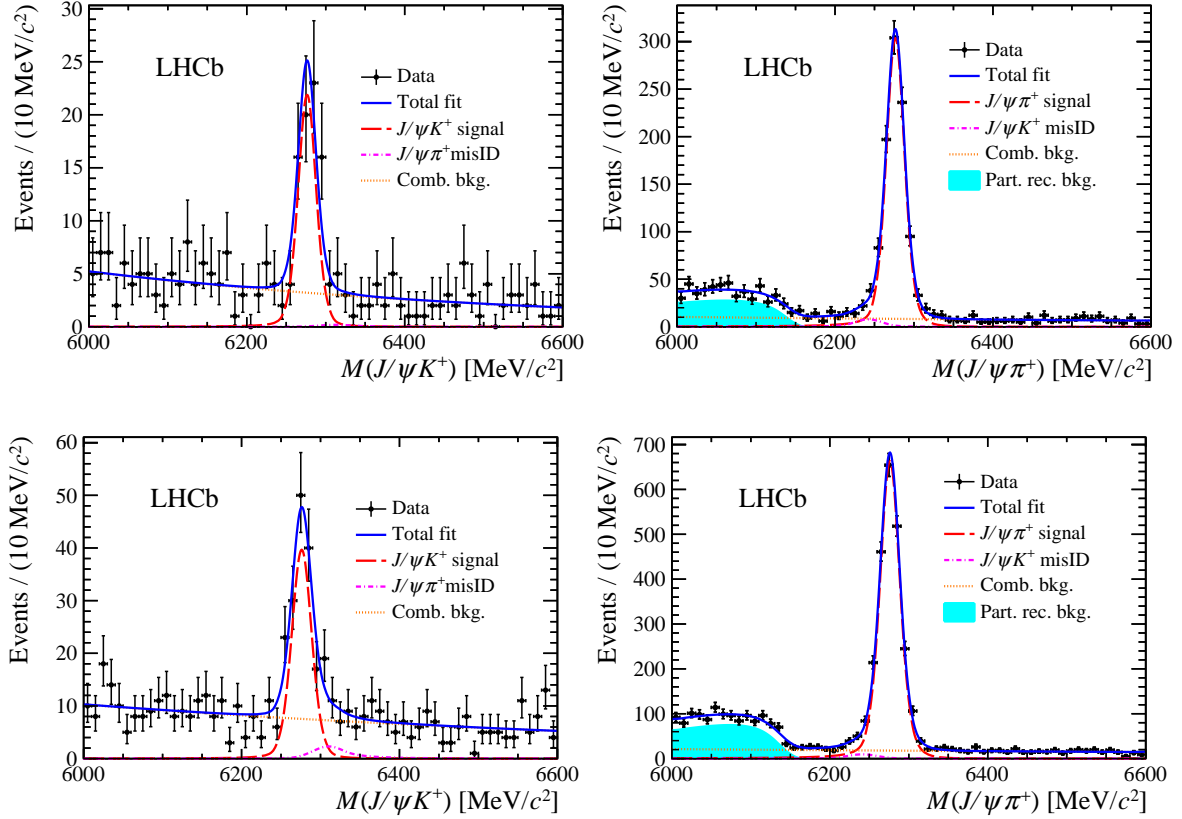


Figure 1: Fits to the reconstructed $B_c^+ \rightarrow J/\psi K^+$ (left) and $B_c^+ \rightarrow J/\psi \pi^+$ (right) mass distributions using 7 TeV (top) and 8 TeV (bottom) data samples. The contributions from the signal, the misidentification background, the combinatorial background and the partially reconstructed background are indicated in the figures.

the combinatorial background changes the mean values of $R_{K/\pi}$ by 1.1% and 0.5% for the two samples.

In the nominal fit, the partially reconstructed background is neglected for $B_c^+ \rightarrow J/\psi K^+$ decays for reasons of fit stability. The associated systematic uncertainties are estimated by including such a component in the same way as was done for $B_c^+ \rightarrow J/\psi \pi^+$ decays, and are found to be 3.3% and 3.2% for the 7 and 8 TeV data, respectively. Using the sum of two DSCB functions instead of a single DSCB function for the misidentification background events changes the mean values of $R_{K/\pi}$ by 0.2% and 0.0% for the two samples.

The selection and trigger efficiencies are calculated with simulated samples. Systematic effects on the efficiency evaluation due to differences between data and simulation in the distributions of variables such as muon momentum and B_c^+ decay time are investigated. Such effects are found to cancel in the efficiency ratio and thus have negligible impact on $R_{K/\pi}$.

The kaon and pion identification efficiencies are measured as functions of momentum and pseudorapidity with a control sample of $D^{*+} \rightarrow D^0 \pi^+$, $D^0 \rightarrow K^- \pi^+$ decays, and represented by two-dimensional histograms. When the histogram binning is varied, the largest changes in the efficiency ratio seen are 0.2% and 0.1% for the 7 TeV and 8 TeV samples, and these values are assigned as the corresponding relative systematic uncertainties.

The simulation accounts for the different interaction cross-sections of pions and kaons with matter. However, if the amount of material in the detector is not modelled correctly, this would alter the efficiency ratio. A systematic uncertainty of 0.3% associated with this effect is assigned for both 7 TeV and 8 TeV samples. Adding all of the above contributions in quadrature, the total relative systematic uncertainties on $R_{K/\pi}$ are 3.5% and 3.4% for the 7 TeV and 8 TeV results.

Table 1: Summary of the relative systematic uncertainties on $R_{K/\pi}$.

	7 TeV	8 TeV
Signal model	0.5%	0.8%
Combinatorial background	1.1%	0.5%
Partially reconstructed background	3.3%	3.2%
Misidentification background	0.2%	0.0%
Particle identification efficiency	0.2%	0.1%
Detector material	0.3%	0.3%
Total	3.5%	3.4%

6 Results and summary

Using the yield and efficiency ratios, the ratio of branching fractions of $B_c^+ \rightarrow J/\psi K^+$ and $B_c^+ \rightarrow J/\psi \pi^+$ is evaluated as

$$R_{K/\pi} = 0.089 \pm 0.013 \pm 0.003$$

for the 7 TeV data sample and

$$R_{K/\pi} = 0.075 \pm 0.008 \pm 0.003$$

for the 8 TeV sample, where the first uncertainties are statistical and the second are systematic.

The two results are combined by evaluating their weighted average. The systematic uncertainties of both measurements are dominated by the contribution from the non-inclusion of the partially reconstructed background for $B_c^+ \rightarrow J/\psi K^+$ decays, and so are assumed to be fully correlated, while their statistical uncertainties are independent. The combined measurement for the 7 TeV and 8 TeV data sample is

$$R_{K/\pi} = 0.079 \pm 0.007 \pm 0.003.$$

This is consistent with the previous LHCb measurement $R_{K/\pi} = 0.069 \pm 0.019 \pm 0.005$ [16], which was based on the 7 TeV data alone. The uncertainties are significantly reduced due to both the increased sample size and the improved event selection. The result supersedes the previous measurement [16] and agrees with the theoretical predictions in Refs. [1, 5–7, 10, 12–15], but disfavours that based on QCD sum rules [11].

Acknowledgements

We express our gratitude to our colleagues in the CERN accelerator departments for the excellent performance of the LHC. We thank the technical and administrative staff at the LHCb institutes. We acknowledge support from CERN and from the national agencies: CAPES, CNPq, FAPERJ and FINEP (Brazil); NSFC (China); CNRS/IN2P3 (France); BMBF, DFG and MPG (Germany); INFN (Italy); FOM and NWO (The Netherlands); MNiSW and NCN (Poland); MEN/IFA (Romania); MinES and FANO (Russia); MinECo (Spain); SNSF and SER (Switzerland); NASU (Ukraine); STFC (United Kingdom); NSF (USA). We acknowledge the computing resources that are provided by CERN, IN2P3 (France), KIT and DESY (Germany), INFN (Italy), SURF (The Netherlands), PIC (Spain), GridPP (United Kingdom), RRCKI and Yandex LLC (Russia), CSCS (Switzerland), IFIN-HH (Romania), CBPF (Brazil), PL-GRID (Poland) and OSC (USA). We are indebted to the communities behind the multiple open source software packages on which we depend. Individual groups or members have received support from AvH Foundation (Germany), EPLANET, Marie Skłodowska-Curie Actions and ERC (European Union), Conseil Général de Haute-Savoie, Labex ENIGMASS and OCEVU, Région Auvergne (France), RFBR and Yandex LLC (Russia), GVA, XuntaGal and GENCAT (Spain), Herchel Smith Fund, The Royal Society, Royal Commission for the Exhibition of 1851 and the Leverhulme Trust (United Kingdom).

References

- [1] V. V. Kiselev, A. E. Kovalsky, and A. K. Likhoded, *B_c decays and lifetime in QCD sum rules*, Nucl. Phys. **B585** (2000) 353, [arXiv:hep-ph/0002127](#).
- [2] B. D. Jones and R. M. Woloshyn, *Mesonic decay constants in lattice NRQCD*, Phys. Rev. **D60** (1999) 014502, [arXiv:hep-lat/9812008](#).
- [3] V. V. Kiselev, A. K. Likhoded, and A. I. Onishchenko, *Semileptonic B_c meson decays in sum rules of QCD and NRQCD*, Nucl. Phys. **B569** (2000) 473, [arXiv:hep-ph/9905359](#).
- [4] E. J. Eichten and C. Quigg, *Mesons with beauty and charm: Spectroscopy*, Phys. Rev. **D49** (1994) 5845, [arXiv:hep-ph/9402210](#).
- [5] S. Naimuddin *et al.*, *Nonleptonic two-body B_c -meson decays*, Phys. Rev. **D86** (2012) 094028.
- [6] C.-H. Chang and Y.-Q. Chen, *Decays of the B_c meson*, Phys. Rev. **D49** (1994) 3399.
- [7] J.-F. Liu and K.-T. Chao, *B_c meson weak decays and CP violation*, Phys. Rev. **D56** (1997) 4133.
- [8] A. Yu. Anisimov, I. M. Narodetsky, C. Semay, and B. Silvestre-Brac, *The B_c meson lifetime in the light front constituent quark model*, Phys. Lett. **B452** (1999) 129, [arXiv:hep-ph/9812514](#).
- [9] P. Colangelo and F. De Fazio, *Using heavy quark spin symmetry in semileptonic B_c decays*, Phys. Rev. **D61** (2000) 034012, [arXiv:hep-ph/9909423](#).

- [10] A. Abd El-Hady, J. H. Munoz, and J. P. Vary, *Semileptonic and nonleptonic B_c decays*, Phys. Rev. **D62** (2000) 014019, arXiv:hep-ph/9909406.
- [11] V. V. Kiselev, *Exclusive decays and lifetime of B_c meson in QCD sum rules*, arXiv:hep-ph/0211021.
- [12] D. Ebert, R. N. Faustov, and V. O. Galkin, *Weak decays of the B_c meson to charmonium and D mesons in the relativistic quark model*, Phys. Rev. **D68** (2003) 094020, arXiv:hep-ph/0306306.
- [13] M. A. Ivanov, J. G. Körner, and P. Santorelli, *Exclusive semileptonic and nonleptonic decays of the B_c meson*, Phys. Rev. **D73** (2006) 054024, arXiv:hep-ph/0602050.
- [14] C.-F. Qiao, P. Sun, D. Yang, and R.-L. Zhu, *B_c exclusive decays to charmonia and light mesons in QCD factorisation at next-to-leading order accuracy*, Phys. Rev. **D89** (2014) 034008, arXiv:1209.5859.
- [15] H.-W. Ke, T. Liu, and X.-Q. Li, *Transitions of $B_c \rightarrow \psi(1S, 2S)$ and the modified harmonic oscillator wave function in LFQM*, Phys. Rev. **D89** (2014) 017501, arXiv:1307.5925.
- [16] LHCb collaboration, R. Aaij *et al.*, *First observation of the decay $B_c^+ \rightarrow J/\psi K^+$* , JHEP **09** (2013) 075, arXiv:1306.6723.
- [17] LHCb collaboration, A. A. Alves Jr. *et al.*, *The LHCb detector at the LHC*, JINST **3** (2008) S08005.
- [18] LHCb collaboration, R. Aaij *et al.*, *LHCb detector performance*, Int. J. Mod. Phys. **A30** (2015) 1530022, arXiv:1412.6352.
- [19] Particle Data Group, K. A. Olive *et al.*, *Review of particle physics*, Chin. Phys. **C38** (2014) 090001, and 2015 update.
- [20] T. Sjöstrand, S. Mrenna, and P. Skands, *PYTHIA 6.4 physics and manual*, JHEP **05** (2006) 026, arXiv:hep-ph/0603175.
- [21] I. Belyaev *et al.*, *Handling of the generation of primary events in Gauss, the LHCb simulation framework*, J. Phys. Conf. Ser. **331** (2011) 032047.
- [22] C.-H. Chang, C. Driouichi, P. Eerola, and X. G. Wu, *BCVEGPY: An event generator for hadronic production of the B_c meson*, Comput. Phys. Commun. **159** (2004) 192, arXiv:hep-ph/0309120.
- [23] C.-H. Chang, J.-X. Wang, and X.-G. Wu, *BCVEGPY2.0: An upgraded version of the generator BCVEGPY with the addition of hadroproduction of the P -wave B_c states*, Comput. Phys. Commun. **174** (2006) 241, arXiv:hep-ph/0504017.
- [24] D. J. Lange, *The EvtGen particle decay simulation package*, Nucl. Instrum. Meth. **A462** (2001) 152.
- [25] P. Golonka and Z. Was, *PHOTOS Monte Carlo: A precision tool for QED corrections in Z and W decays*, Eur. Phys. J. **C45** (2006) 97, arXiv:hep-ph/0506026.

- [26] Geant4 collaboration, J. Allison *et al.*, *Geant4 developments and applications*, IEEE Trans. Nucl. Sci. **53** (2006) 270; Geant4 collaboration, S. Agostinelli *et al.*, *Geant4: A simulation toolkit*, Nucl. Instrum. Meth. **A506** (2003) 250.
- [27] M. Clemencic *et al.*, *The LHCb simulation application, Gauss: Design, evolution and experience*, J. Phys. Conf. Ser. **331** (2011) 032023.
- [28] L. Breiman, J. H. Friedman, R. A. Olshen, and C. J. Stone, *Classification and regression trees*, Wadsworth international group, Belmont, California, USA, 1984.
- [29] ARGUS collaboration, H. Albrecht *et al.*, *Search for hadronic $b \rightarrow u$ decays*, Phys. Lett. **B241** (1990) 278.

LHCb collaboration

R. Aaij³⁹, B. Adeva³⁸, M. Adinolfi⁴⁷, Z. Ajaltouni⁵, S. Akar⁶, J. Albrecht¹⁰, F. Alessio³⁹, M. Alexander⁵², S. Ali⁴², G. Alkhazov³¹, P. Alvarez Cartelle⁵⁴, A.A. Alves Jr⁵⁸, S. Amato², S. Amerio²³, Y. Amhis⁷, L. An⁴⁰, L. Anderlini¹⁸, G. Andreassi⁴⁰, M. Andreotti^{17,g}, J.E. Andrews⁵⁹, R.B. Appleby⁵⁵, O. Aquines Gutierrez¹¹, F. Archilli¹, P. d'Argent¹², J. Arnau Romeu⁶, A. Artamonov³⁶, M. Artuso⁶⁰, E. Aslanides⁶, G. Auriemma²⁶, M. Baalouch⁵, I. Babuschkin⁵⁵, S. Bachmann¹², J.J. Back⁴⁹, A. Badalov³⁷, C. Baesso⁶¹, W. Baldini¹⁷, R.J. Barlow⁵⁵, C. Barschel³⁹, S. Barsuk⁷, W. Barter³⁹, V. Batozskaya²⁹, B. Batsukh⁶⁰, V. Battista⁴⁰, A. Bay⁴⁰, L. Beaucourt⁴, J. Beddow⁵², F. Bedeschi²⁴, I. Bediaga¹, L.J. Bel⁴², V. Bellee⁴⁰, N. Belloli^{21,i}, K. Belous³⁶, I. Belyaev³², E. Ben-Haim⁸, G. Bencivenni¹⁹, S. Benson³⁹, J. Benton⁴⁷, A. Berezhnoy³³, R. Bernet⁴¹, A. Bertolin²³, F. Betti¹⁵, M.-O. Bettler³⁹, M. van Beuzekom⁴², I. Bezshyiko⁴¹, S. Bifani⁴⁶, P. Billoir⁸, T. Bird⁵⁵, A. Birnkraut¹⁰, A. Bitadze⁵⁵, A. Bizzeti^{18,u}, T. Blake⁴⁹, F. Blanc⁴⁰, J. Blouw¹¹, S. Blusk⁶⁰, V. Bocci²⁶, T. Boettcher⁵⁷, A. Bondar³⁵, N. Bondar^{31,39}, W. Bonivento¹⁶, A. Borgheresi^{21,i}, S. Borghi⁵⁵, M. Borisov⁶⁷, M. Borsato³⁸, F. Bossu⁷, M. Boubdir⁹, T.J.V. Bowcock⁵³, E. Bowen⁴¹, C. Bozzi^{17,39}, S. Braun¹², M. Britsch¹², T. Britton⁶⁰, J. Brodzicka⁵⁵, E. Buchanan⁴⁷, C. Burr⁵⁵, A. Bursche², J. Buytaert³⁹, S. Cadeddu¹⁶, R. Calabrese^{17,g}, M. Calvi^{21,i}, M. Calvo Gomez^{37,m}, P. Campana¹⁹, D. Campora Perez³⁹, L. Capriotti⁵⁵, A. Carbone^{15,e}, G. Carboni^{25,j}, R. Cardinale^{20,h}, A. Cardini¹⁶, P. Carniti^{21,i}, L. Carson⁵¹, K. Carvalho Akiba², G. Casse⁵³, L. Cassina^{21,i}, L. Castillo Garcia⁴⁰, M. Cattaneo³⁹, Ch. Cauet¹⁰, G. Cavallero²⁰, R. Cenci^{24,t}, M. Charles⁸, Ph. Charpentier³⁹, G. Chatzikonstantinidis⁴⁶, M. Chefdeville⁴, S. Chen⁵⁵, S.-F. Cheung⁵⁶, V. Chobanova³⁸, M. Chruszcz^{41,27}, X. Cid Vidal³⁸, G. Ciezarek⁴², P.E.L. Clarke⁵¹, M. Clemencic³⁹, H.V. Cliff⁴⁸, J. Closier³⁹, V. Coco⁵⁸, J. Cogan⁶, E. Cogneras⁵, V. Cogoni^{16,39,f}, L. Cojocariu³⁰, G. Collazuol^{23,o}, P. Collins³⁹, A. Comerma-Montells¹², A. Contu³⁹, A. Cook⁴⁷, S. Coquereau⁸, G. Corti³⁹, M. Corvo^{17,g}, C.M. Costa Sobral⁴⁹, B. Couturier³⁹, G.A. Cowan⁵¹, D.C. Craik⁵¹, A. Crocombe⁴⁹, M. Cruz Torres⁶¹, S. Cunliffe⁵⁴, R. Currie⁵⁴, C. D'Ambrosio³⁹, E. Dall'Occo⁴², J. Dalseno⁴⁷, P.N.Y. David⁴², A. Davis⁵⁸, O. De Aguiar Francisco², K. De Bruyn⁶, S. De Capua⁵⁵, M. De Cian¹², J.M. De Miranda¹, L. De Paula², M. De Serio^{14,d}, P. De Simone¹⁹, C.-T. Dean⁵², D. Decamp⁴, M. Deckenhoff¹⁰, L. Del Buono⁸, M. Demmer¹⁰, D. Derkach⁶⁷, O. Deschamps⁵, F. Dettori³⁹, B. Dey²², A. Di Canto³⁹, H. Dijkstra³⁹, F. Dordei³⁹, M. Dorigo⁴⁰, A. Dosil Suárez³⁸, A. Dovbnya⁴⁴, K. Dreimanis⁵³, L. Dufour⁴², G. Dujany⁵⁵, K. Dungs³⁹, P. Durante³⁹, R. Dzhelyadin³⁶, A. Dziurda³⁹, A. Dzyuba³¹, N. Déleage⁴, S. Easo⁵⁰, U. Egede⁵⁴, V. Egorychev³², S. Eidelman³⁵, S. Eisenhardt⁵¹, U. Eitschberger¹⁰, R. Ekelhof¹⁰, L. Eklund⁵², Ch. Elsasser⁴¹, S. Ely⁶⁰, S. Esen¹², H.M. Evans⁴⁸, T. Evans⁵⁶, A. Falabella¹⁵, N. Farley⁴⁶, S. Farry⁵³, R. Fay⁵³, D. Fazzini^{21,i}, D. Ferguson⁵¹, V. Fernandez Albor³⁸, F. Ferrari^{15,39}, F. Ferreira Rodrigues¹, M. Ferro-Luzzi³⁹, S. Filippov³⁴, R.A. Fini¹⁴, M. Fiore^{17,g}, M. Fiorini^{17,g}, M. Firlej²⁸, C. Fitzpatrick⁴⁰, T. Fiutowski²⁸, F. Fleuret^{7,b}, K. Fohl³⁹, M. Fontana¹⁶, F. Fontanelli^{20,h}, D.C. Forshaw⁶⁰, R. Forty³⁹, V. Franco Lima⁵³, M. Frank³⁹, C. Frei³⁹, J. Fu^{22,q}, E. Furfaro^{25,j}, C. Färber³⁹, A. Gallas Torreira³⁸, D. Galli^{15,e}, S. Gallorini²³, S. Gambetta⁵¹, M. Gandelman², P. Gandini⁵⁶, Y. Gao³, J. García Pardiñas³⁸, J. Garra Tico⁴⁸, L. Garrido³⁷, P.J. Garsed⁴⁸, D. Gascon³⁷, C. Gaspar³⁹, L. Gavardi¹⁰, G. Gazzoni⁵, D. Gerick¹², E. Gersabeck¹², M. Gersabeck⁵⁵, T. Gershon⁴⁹, Ph. Ghez⁴, S. Giani⁴⁰, V. Gibson⁴⁸, O.G. Girard⁴⁰, L. Giubega³⁰, K. Gizdov⁵¹, V.V. Gligorov⁸, D. Golubkov³², A. Golutvin^{54,39}, A. Gomes^{1,a}, I.V. Gorelov³³, C. Gotti^{21,i}, M. Grabalosa Gándara⁵, R. Graciani Diaz³⁷, L.A. Granado Cardoso³⁹, E. Graugés³⁷, E. Graverini⁴¹, G. Graziani¹⁸, A. Greco³⁰, P. Griffith⁴⁶, L. Grillo²¹, B.R. Gruber Cazon⁵⁶, O. Grünberg⁶⁵, E. Gushchin³⁴, Yu. Guz³⁶, T. Gys³⁹, C. Göbel⁶¹, T. Hadavizadeh⁵⁶, C. Hadjivasiliou⁵, G. Haefeli⁴⁰, C. Haen³⁹, S.C. Haines⁴⁸, S. Hall⁵⁴, B. Hamilton⁵⁹, X. Han¹², S. Hansmann-Menzemer¹², N. Harnew⁵⁶, S.T. Harnew⁴⁷,

J. Harrison⁵⁵, M. Hatch³⁹, J. He⁶², T. Head⁴⁰, A. Heister⁹, K. Hennessy⁵³, P. Henrard⁵,
 L. Henry⁸, J.A. Hernando Morata³⁸, E. van Herwijnen³⁹, M. Heß⁶⁵, A. Hicheur², D. Hill⁵⁶,
 C. Hombach⁵⁵, W. Hulsbergen⁴², T. Humair⁵⁴, M. Hushchyn⁶⁷, N. Hussain⁵⁶, D. Hutchcroft⁵³,
 M. Idzik²⁸, P. Ilten⁵⁷, R. Jacobsson³⁹, A. Jaeger¹², J. Jalocha⁵⁶, E. Jans⁴², A. Jawahery⁵⁹,
 M. John⁵⁶, D. Johnson³⁹, C.R. Jones⁴⁸, C. Joram³⁹, B. Jost³⁹, N. Jurik⁶⁰, S. Kandybei⁴⁴,
 W. Kalso⁶, M. Karacson³⁹, J.M. Kariuki⁴⁷, S. Karodia⁵², M. Kecke¹², M. Kelsey⁶⁰,
 I.R. Kenyon⁴⁶, M. Kenzie³⁹, T. Ketel⁴³, E. Khairullin⁶⁷, B. Khanji^{21,39,i}, C. Khurewathanakul⁴⁰,
 T. Kirn⁹, S. Klaver⁵⁵, K. Klimaszewski²⁹, S. Koliiev⁴⁵, M. Kolpin¹², I. Komarov⁴⁰,
 R.F. Koopman⁴³, P. Koppenburg⁴², A. Kozachuk³³, M. Kozeiha⁵, L. Kravchuk³⁴, K. Kreplin¹²,
 M. Kreps⁴⁹, P. Krokovny³⁵, F. Kruse¹⁰, W. Krzemien²⁹, W. Kucewicz^{27,l}, M. Kucharczyk²⁷,
 V. Kudryavtsev³⁵, A.K. Kuonen⁴⁰, K. Kurek²⁹, T. Kvaratskheliya^{32,39}, D. Lacarrere³⁹,
 G. Lafferty^{55,39}, A. Lai¹⁶, D. Lambert⁵¹, G. Lanfranchi¹⁹, C. Langenbruch⁹, B. Langhans³⁹,
 T. Latham⁴⁹, C. Lazzeroni⁴⁶, R. Le Gac⁶, J. van Leerdam⁴², J.-P. Lees⁴, A. Leflat^{33,39},
 J. Lefrançois⁷, R. Lefèvre⁵, F. Lemaitre³⁹, E. Lemos Cid³⁸, O. Leroy⁶, T. Lesiak²⁷,
 B. Leverington¹², Y. Li⁷, T. Likhomanenko^{67,66}, R. Lindner³⁹, C. Linn³⁹, F. Lionetto⁴¹,
 B. Liu¹⁶, X. Liu³, D. Loh⁴⁹, I. Longstaff⁵², J.H. Lopes², D. Lucchesi^{23,o}, M. Lucio Martinez³⁸,
 H. Luo⁵¹, A. Lupato²³, E. Luppi^{17,g}, O. Lupton⁵⁶, A. Lusiani²⁴, X. Lyu⁶², F. Machefert⁷,
 F. Maciuc³⁰, O. Maev³¹, K. Maguire⁵⁵, S. Malde⁵⁶, A. Malinin⁶⁶, T. Maltsev³⁵, G. Manca⁷,
 G. Mancinelli⁶, P. Manning⁶⁰, J. Maratas^{5,v}, J.F. Marchand⁴, U. Marconi¹⁵, C. Marin Benito³⁷,
 P. Marino^{24,t}, J. Marks¹², G. Martellotti²⁶, M. Martin⁶, M. Martinelli⁴⁰, D. Martinez Santos³⁸,
 F. Martinez Vidal⁶⁸, D. Martins Tostes², L.M. Massacrier⁷, A. Massafferri¹, R. Matev³⁹,
 A. Mathad⁴⁹, Z. Mathe³⁹, C. Matteuzzi²¹, A. Mauri⁴¹, B. Maurin⁴⁰, A. Mazurov⁴⁶,
 M. McCann⁵⁴, J. McCarthy⁴⁶, A. McNab⁵⁵, R. McNulty¹³, B. Meadows⁵⁸, F. Meier¹⁰,
 M. Meissner¹², D. Melnychuk²⁹, M. Merk⁴², A. Merli^{22,q}, E. Michielin²³, D.A. Milanese⁶⁴,
 M.-N. Minard⁴, D.S. Mitzel¹², J. Molina Rodriguez⁶¹, I.A. Monroy⁶⁴, S. Monteil⁵,
 M. Morandin²³, P. Morawski²⁸, A. Mordà⁶, M.J. Morello^{24,t}, J. Moron²⁸, A.B. Morris⁵¹,
 R. Mountain⁶⁰, F. Muheim⁵¹, M. Mulder⁴², M. Mussini¹⁵, D. Müller⁵⁵, J. Müller¹⁰, K. Müller⁴¹,
 V. Müller¹⁰, P. Naik⁴⁷, T. Nakada⁴⁰, R. Nandakumar⁵⁰, A. Nandi⁵⁶, I. Nasteva²,
 M. Needham⁵¹, N. Neri²², S. Neubert¹², N. Neufeld³⁹, M. Neuner¹², A.D. Nguyen⁴⁰,
 C. Nguyen-Mau^{40,n}, S. Nieswand⁹, R. Niet¹⁰, N. Nikitin³³, T. Nikodem¹², A. Novoselov³⁶,
 D.P. O'Hanlon⁴⁹, A. Oblakowska-Mucha²⁸, V. Obraztsov³⁶, S. Ogilvy¹⁹, R. Oldeman⁴⁸,
 C.J.G. Onderwater⁶⁹, J.M. Otalora Goicochea², A. Otto³⁹, P. Owen⁴¹, A. Oyanguren⁶⁸,
 P.R. Pais⁴⁰, A. Palano^{14,d}, F. Palombo^{22,q}, M. Palutan¹⁹, J. Panman³⁹, A. Papanestis⁵⁰,
 M. Pappagallo^{14,d}, L.L. Pappalardo^{17,g}, C. Pappenheimer⁵⁸, W. Parker⁵⁹, C. Parkes⁵⁵,
 G. Passaleva¹⁸, A. Pastore^{14,d}, G.D. Patel⁵³, M. Patel⁵⁴, C. Patrignani^{15,e}, A. Pearce^{55,50},
 A. Pellegrino⁴², G. Penso^{26,k}, M. Pepe Altarelli³⁹, S. Perazzini³⁹, P. Perret⁵, L. Pescatore⁴⁶,
 K. Petridis⁴⁷, A. Petrolini^{20,h}, A. Petrov⁶⁶, M. Petruzzo^{22,q}, E. Picatoste Olloqui³⁷,
 B. Pietrzyk⁴, M. Pikies²⁷, D. Pinci²⁶, A. Pistone²⁰, A. Piucci¹², S. Playfer⁵¹, M. Plo Casasus³⁸,
 T. Poikela³⁹, F. Polci⁸, A. Poluektov^{49,35}, I. Polyakov⁶⁰, E. Polycarpo², G.J. Pomery⁴⁷,
 A. Popov³⁶, D. Popov^{11,39}, B. Popovici³⁰, C. Potterat², E. Price⁴⁷, J.D. Price⁵³,
 J. Prisciandaro³⁸, A. Pritchard⁵³, C. Prouve⁴⁷, V. Pugatch⁴⁵, A. Puig Navarro⁴⁰, G. Punzi^{24,p},
 W. Qian⁵⁶, R. Quagliani^{7,47}, B. Rachwal²⁷, J.H. Rademacker⁴⁷, M. Rama²⁴,
 M. Ramos Pernas³⁸, M.S. Rangel², I. Raniuk⁴⁴, G. Raven⁴³, F. Redi⁵⁴, S. Reichert¹⁰,
 A.C. dos Reis¹, C. Remon Alepuz⁶⁸, V. Renaudin⁷, S. Ricciardi⁵⁰, S. Richards⁴⁷, M. Rihl³⁹,
 K. Rinnert^{53,39}, V. Rives Molina³⁷, P. Robbe^{7,39}, A.B. Rodrigues¹, E. Rodrigues⁵⁸,
 J.A. Rodriguez Lopez⁶⁴, P. Rodriguez Perez⁵⁵, A. Rogozhnikov⁶⁷, S. Roiser³⁹,
 V. Romanovskiy³⁶, A. Romero Vidal³⁸, J.W. Ronayne¹³, M. Rotondo²³, M.S. Rudolph⁶⁰,
 T. Ruf³⁹, P. Ruiz Valls⁶⁸, J.J. Saborido Silva³⁸, E. Sadykhov³², N. Sagidova³¹, B. Saitta^{16,f},
 V. Salustino Guimaraes², C. Sanchez Mayordomo⁶⁸, B. Sanmartin Sedes³⁸, R. Santacesaria²⁶,
 C. Santamarina Rios³⁸, M. Santimaria¹⁹, E. Santovetti^{25,j}, A. Sarti^{19,k}, C. Satriano^{26,s},

A. Satta²⁵, D.M. Saunders⁴⁷, D. Savrina^{32,33}, S. Schael⁹, M. Schellenberg¹⁰, M. Schiller³⁹, H. Schindler³⁹, M. Schlupp¹⁰, M. Schmelling¹¹, T. Schmelzer¹⁰, B. Schmidt³⁹, O. Schneider⁴⁰, A. Schopper³⁹, K. Schubert¹⁰, M. Schubiger⁴⁰, M.-H. Schune⁷, R. Schwemmer³⁹, B. Sciascia¹⁹, A. Sciubba^{26,k}, A. Semennikov³², A. Sergi⁴⁶, N. Serra⁴¹, J. Serrano⁶, L. Sestini²³, P. Seyfert²¹, M. Shapkin³⁶, I. Shapoval^{17,44,g}, Y. Shcheglov³¹, T. Shears⁵³, L. Shekhtman³⁵, V. Shevchenko⁶⁶, A. Shires¹⁰, B.G. Siddi¹⁷, R. Silva Coutinho⁴¹, L. Silva de Oliveira², G. Simi^{23,o}, S. Simone^{14,d}, M. Sirendi⁴⁸, N. Skidmore⁴⁷, T. Skwarnicki⁶⁰, E. Smith⁵⁴, I.T. Smith⁵¹, J. Smith⁴⁸, M. Smith⁵⁵, H. Snoek⁴², M.D. Sokoloff⁵⁸, F.J.P. Soler⁵², D. Souza⁴⁷, B. Souza De Paula², B. Spaan¹⁰, P. Spradlin⁵², S. Sridharan³⁹, F. Stagni³⁹, M. Stahl¹², S. Stahl³⁹, P. Stefko⁴⁰, S. Stefkova⁵⁴, O. Steinkamp⁴¹, S. Stemmler¹², O. Stenyakin³⁶, S. Stevenson⁵⁶, S. Stoica³⁰, S. Stone⁶⁰, B. Storaci⁴¹, S. Stracka^{24,t}, M. Straticiu³⁰, U. Straumann⁴¹, L. Sun⁵⁸, W. Sutcliffe⁵⁴, K. Swientek²⁸, V. Syropoulos⁴³, M. Szczekowski²⁹, T. Szumlak²⁸, S. T'Jampens⁴, A. Tayduganov⁶, T. Tekampe¹⁰, G. Tellarini^{17,g}, F. Teubert³⁹, C. Thomas⁵⁶, E. Thomas³⁹, J. van Tilburg⁴², V. Tisserand⁴, M. Tobin⁴⁰, S. Tolk⁴⁸, L. Tomassetti^{17,g}, D. Tonelli³⁹, S. Topp-Joergensen⁵⁶, F. Toriello⁶⁰, E. Tournefier⁴, S. Tourneur⁴⁰, K. Trabelsi⁴⁰, M. Traill⁵², M.T. Tran⁴⁰, M. Tresch⁴¹, A. Trisovic³⁹, A. Tsaregorodtsev⁶, P. Tsopelas⁴², A. Tully⁴⁸, N. Tuning⁴², A. Ukleja²⁹, A. Ustyuzhanin^{67,66}, U. Uwer¹², C. Vacca^{16,39,f}, V. Vagnoni^{15,39}, S. Valat³⁹, G. Valenti¹⁵, A. Vallier⁷, R. Vazquez Gomez¹⁹, P. Vazquez Regueiro³⁸, S. Vecchi¹⁷, M. van Veghel⁴², J.J. Velthuis⁴⁷, M. Veltri^{18,r}, G. Veneziano⁴⁰, A. Venkateswaran⁶⁰, M. Vernet⁵, M. Vesterinen¹², B. Viaud⁷, D. Vieira¹, M. Vieites Diaz³⁸, X. Vilasis-Cardona^{37,m}, V. Volkov³³, A. Vollhardt⁴¹, B. Voneki³⁹, D. Voong⁴⁷, A. Vorobyev³¹, V. Vorobyev³⁵, C. Voß⁶⁵, J.A. de Vries⁴², C. Vázquez Sierra³⁸, R. Waldi⁶⁵, C. Wallace⁴⁹, R. Wallace¹³, J. Walsh²⁴, J. Wang⁶⁰, D.R. Ward⁴⁸, H.M. Wark⁵³, N.K. Watson⁴⁶, D. Websdale⁵⁴, A. Weiden⁴¹, M. Whitehead³⁹, J. Wicht⁴⁹, G. Wilkinson^{56,39}, M. Wilkinson⁶⁰, M. Williams³⁹, M.P. Williams⁴⁶, M. Williams⁵⁷, T. Williams⁴⁶, F.F. Wilson⁵⁰, J. Wimberley⁵⁹, J. Wishahi¹⁰, W. Wislicki²⁹, M. Witek²⁷, G. Wormser⁷, S.A. Wotton⁴⁸, K. Wraight⁵², S. Wright⁴⁸, K. Wyllie³⁹, Y. Xie⁶³, Z. Xing⁶⁰, Z. Xu⁴⁰, Z. Yang³, H. Yin⁶³, J. Yu⁶³, X. Yuan³⁵, O. Yushchenko³⁶, M. Zangoli¹⁵, K.A. Zarebski⁴⁶, M. Zavertyaev^{11,c}, L. Zhang³, Y. Zhang⁷, Y. Zhang⁶², A. Zhelezov¹², Y. Zheng⁶², A. Zhokhov³², X. Zhu³, V. Zhukov⁹, S. Zucchelli¹⁵.

¹Centro Brasileiro de Pesquisas Físicas (CBPF), Rio de Janeiro, Brazil

²Universidade Federal do Rio de Janeiro (UFRJ), Rio de Janeiro, Brazil

³Center for High Energy Physics, Tsinghua University, Beijing, China

⁴LAPP, Université Savoie Mont-Blanc, CNRS/IN2P3, Annecy-Le-Vieux, France

⁵Clermont Université, Université Blaise Pascal, CNRS/IN2P3, LPC, Clermont-Ferrand, France

⁶CPPM, Aix-Marseille Université, CNRS/IN2P3, Marseille, France

⁷LAL, Université Paris-Sud, CNRS/IN2P3, Orsay, France

⁸LPNHE, Université Pierre et Marie Curie, Université Paris Diderot, CNRS/IN2P3, Paris, France

⁹I. Physikalisches Institut, RWTH Aachen University, Aachen, Germany

¹⁰Fakultät Physik, Technische Universität Dortmund, Dortmund, Germany

¹¹Max-Planck-Institut für Kernphysik (MPIK), Heidelberg, Germany

¹²Physikalisches Institut, Ruprecht-Karls-Universität Heidelberg, Heidelberg, Germany

¹³School of Physics, University College Dublin, Dublin, Ireland

¹⁴Sezione INFN di Bari, Bari, Italy

¹⁵Sezione INFN di Bologna, Bologna, Italy

¹⁶Sezione INFN di Cagliari, Cagliari, Italy

¹⁷Sezione INFN di Ferrara, Ferrara, Italy

¹⁸Sezione INFN di Firenze, Firenze, Italy

¹⁹Laboratori Nazionali dell'INFN di Frascati, Frascati, Italy

²⁰Sezione INFN di Genova, Genova, Italy

²¹Sezione INFN di Milano Bicocca, Milano, Italy

²²Sezione INFN di Milano, Milano, Italy

²³Sezione INFN di Padova, Padova, Italy

- ²⁴ *Sezione INFN di Pisa, Pisa, Italy*
- ²⁵ *Sezione INFN di Roma Tor Vergata, Roma, Italy*
- ²⁶ *Sezione INFN di Roma La Sapienza, Roma, Italy*
- ²⁷ *Henryk Niewodniczanski Institute of Nuclear Physics Polish Academy of Sciences, Kraków, Poland*
- ²⁸ *AGH - University of Science and Technology, Faculty of Physics and Applied Computer Science, Kraków, Poland*
- ²⁹ *National Center for Nuclear Research (NCBJ), Warsaw, Poland*
- ³⁰ *Horia Hulubei National Institute of Physics and Nuclear Engineering, Bucharest-Magurele, Romania*
- ³¹ *Petersburg Nuclear Physics Institute (PNPI), Gatchina, Russia*
- ³² *Institute of Theoretical and Experimental Physics (ITEP), Moscow, Russia*
- ³³ *Institute of Nuclear Physics, Moscow State University (SINP MSU), Moscow, Russia*
- ³⁴ *Institute for Nuclear Research of the Russian Academy of Sciences (INR RAN), Moscow, Russia*
- ³⁵ *Budker Institute of Nuclear Physics (SB RAS) and Novosibirsk State University, Novosibirsk, Russia*
- ³⁶ *Institute for High Energy Physics (IHEP), Protvino, Russia*
- ³⁷ *ICCUB, Universitat de Barcelona, Barcelona, Spain*
- ³⁸ *Universidad de Santiago de Compostela, Santiago de Compostela, Spain*
- ³⁹ *European Organization for Nuclear Research (CERN), Geneva, Switzerland*
- ⁴⁰ *Ecole Polytechnique Fédérale de Lausanne (EPFL), Lausanne, Switzerland*
- ⁴¹ *Physik-Institut, Universität Zürich, Zürich, Switzerland*
- ⁴² *Nikhef National Institute for Subatomic Physics, Amsterdam, The Netherlands*
- ⁴³ *Nikhef National Institute for Subatomic Physics and VU University Amsterdam, Amsterdam, The Netherlands*
- ⁴⁴ *NSC Kharkiv Institute of Physics and Technology (NSC KIPT), Kharkiv, Ukraine*
- ⁴⁵ *Institute for Nuclear Research of the National Academy of Sciences (KINR), Kyiv, Ukraine*
- ⁴⁶ *University of Birmingham, Birmingham, United Kingdom*
- ⁴⁷ *H.H. Wills Physics Laboratory, University of Bristol, Bristol, United Kingdom*
- ⁴⁸ *Cavendish Laboratory, University of Cambridge, Cambridge, United Kingdom*
- ⁴⁹ *Department of Physics, University of Warwick, Coventry, United Kingdom*
- ⁵⁰ *STFC Rutherford Appleton Laboratory, Didcot, United Kingdom*
- ⁵¹ *School of Physics and Astronomy, University of Edinburgh, Edinburgh, United Kingdom*
- ⁵² *School of Physics and Astronomy, University of Glasgow, Glasgow, United Kingdom*
- ⁵³ *Oliver Lodge Laboratory, University of Liverpool, Liverpool, United Kingdom*
- ⁵⁴ *Imperial College London, London, United Kingdom*
- ⁵⁵ *School of Physics and Astronomy, University of Manchester, Manchester, United Kingdom*
- ⁵⁶ *Department of Physics, University of Oxford, Oxford, United Kingdom*
- ⁵⁷ *Massachusetts Institute of Technology, Cambridge, MA, United States*
- ⁵⁸ *University of Cincinnati, Cincinnati, OH, United States*
- ⁵⁹ *University of Maryland, College Park, MD, United States*
- ⁶⁰ *Syracuse University, Syracuse, NY, United States*
- ⁶¹ *Pontifícia Universidade Católica do Rio de Janeiro (PUC-Rio), Rio de Janeiro, Brazil, associated to ²*
- ⁶² *University of Chinese Academy of Sciences, Beijing, China, associated to ³*
- ⁶³ *Institute of Particle Physics, Central China Normal University, Wuhan, Hubei, China, associated to ³*
- ⁶⁴ *Departamento de Física, Universidad Nacional de Colombia, Bogota, Colombia, associated to ⁸*
- ⁶⁵ *Institut für Physik, Universität Rostock, Rostock, Germany, associated to ¹²*
- ⁶⁶ *National Research Centre Kurchatov Institute, Moscow, Russia, associated to ³²*
- ⁶⁷ *Yandex School of Data Analysis, Moscow, Russia, associated to ³²*
- ⁶⁸ *Instituto de Física Corpuscular (IFIC), Universitat de Valencia-CSIC, Valencia, Spain, associated to ³⁷*
- ⁶⁹ *Van Swinderen Institute, University of Groningen, Groningen, The Netherlands, associated to ⁴²*

^a *Universidade Federal do Triângulo Mineiro (UFTM), Uberaba-MG, Brazil*

^b *Laboratoire Leprince-Ringuet, Palaiseau, France*

^c *P.N. Lebedev Physical Institute, Russian Academy of Science (LPI RAS), Moscow, Russia*

^d *Università di Bari, Bari, Italy*

^e *Università di Bologna, Bologna, Italy*

^f *Università di Cagliari, Cagliari, Italy*

^g *Università di Ferrara, Ferrara, Italy*

^h *Università di Genova, Genova, Italy*

ⁱ *Università di Milano Bicocca, Milano, Italy*

^j *Università di Roma Tor Vergata, Roma, Italy*

^k *Università di Roma La Sapienza, Roma, Italy*

^l *AGH - University of Science and Technology, Faculty of Computer Science, Electronics and Telecommunications, Kraków, Poland*

^m *LIFAEELS, La Salle, Universitat Ramon Llull, Barcelona, Spain*

ⁿ *Hanoi University of Science, Hanoi, Viet Nam*

^o *Università di Padova, Padova, Italy*

^p *Università di Pisa, Pisa, Italy*

^q *Università degli Studi di Milano, Milano, Italy*

^r *Università di Urbino, Urbino, Italy*

^s *Università della Basilicata, Potenza, Italy*

^t *Scuola Normale Superiore, Pisa, Italy*

^u *Università di Modena e Reggio Emilia, Modena, Italy*

^v *Iligan Institute of Technology (IIT), Iligan, Philippines*